N-[2-Methyl-5-(triazol-1-yl)phenyl]pyrimidin-2-amine as a Scaffold for the Synthesis of Inhibitors of Bcr-Abl

ARTICLE *in* CHEMMEDCHEM · NOVEMBER 2011

Impact Factor: 2.97 · DOI: 10.1002/cmdc.201100304 · Source: PubMed

DOI: 10.1002/cmdc.201100304

N-[2-Methyl-5-(triazol-1-yl)phenyl]pyrimidin-2-amine as a Scaffold for the Synthesis of Inhibitors of Bcr-Abl

Federica Arioli,[a] Stella Borrelli,[a] Francesco Colombo,[a] Federico Falchi,[b] Irene Filippi,[c] Emmanuele Crespan,[d] Antonella Naldini,[c] Giusy Scalia,[c] Alessandra Silvani,[a] Giovanni Maga,[d] Fabio Carraro,[c] Maurizio Botta,[b] and Daniele Passarella*[a]

N-[2-Methyl-5-(triazol-1-yl)phenyl]pyrimidin-2-amine derivatives were synthesized and evaluated in vitro for their potential use as inhibitors of Bcr-Abl. The design is based on the bioisosterism between the 1,2,3-triazole ring and the amide group. The synthesis involves a copper(I)-catalyzed azide–alkyne cycloaddition (CuAAC) as the key step, with the exclusive production of *anti*-(1,4)-triazole derivatives. One of the compounds obtained shows general activity similar to that of imatinib; in particular, it was observed to be more effective in decreasing the fundamental function of cdc25A phosphatases in the K-562 cell line.

Introduction

Chronic myelogenous leukemia (CML) is a disease characterized by the presence of the Philadelphia chromosome (discovered in 1960 by Nowell and Hungerford)[1] that results from reciprocal translocation between chromosomes 9 and 22.[2] This translocation fuses the breakpoint cluster region (*Bcr*) and the Abelson kinase (*Abl*) genes, forming the *Bcr-Abl* oncogene,[3] which encodes the constitutively active cytoplasmic tyrosine kinase (TK) Bcr-Abl, present in >90% of CML cases.[4] As a consequence of this fusion, proliferation and viability of myeloid lineage cells is enhanced, and the disease progresses through its three phases—chronic proliferative, accelerated, and blast crisis phase—becoming more resistant to treatment in each successive phase. The findings that Bcr-Abl is the cause of the leukemic phenotype and that the tyrosine kinase activity of Abl is fundamental for Bcr-Abl-mediated transformation have made this kinase an important target for the development of specific therapies. In the recent past, advances in the selective inhibition of Bcr-Abl kinase activity led to the development of several active compounds (Figure 1),[5] and in particular, imatinib mesylate (Gleevec) is the one that currently represents the first-line treatment of CML. However, resistance to imatinib has been conferred by *Bcr-Abl* gene amplification leading to overexpression of the Bcr-Abl protein, point mutations in the Bcr-Abl kinase domain that interfere with imatinib binding, as well as point mutations outside the kinase domain that allosterically inhibit imatinib binding to Bcr-Abl. As a consequence, there is growing interest in the de-

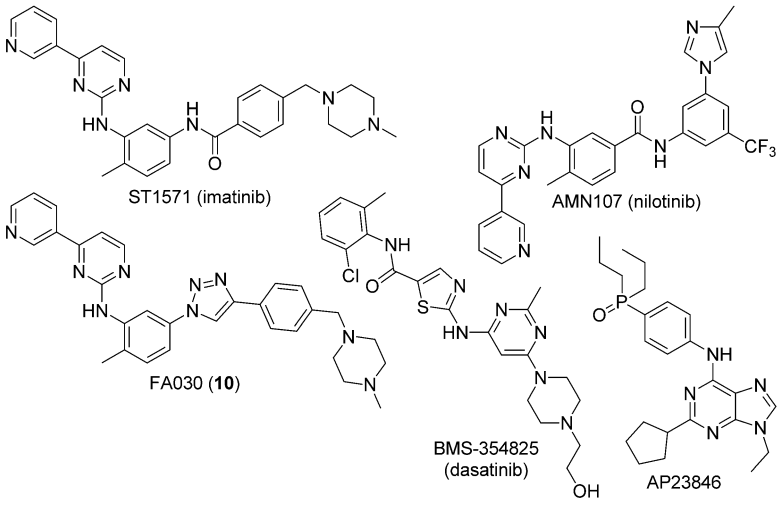

Figure 1. Some available inhibitors of Abl and our Abl inhibitor, FA030 (**10**).

[a] *Dr. F. Arioli, Dr. S. Borrelli, Dr. F. Colombo, Dr. A. Silvani, Prof. Dr. D. Passarella*
Dipartimento di Chimica Organica e Industriale
Università degli Studi di Milan
Via G. Venezian 21, 20133 Milano (Italy)
E-mail: daniele.passarella@unimi.it

[b] *Dr. F. Falchi, Prof. Dr. M. Botta*
Dipartimento Farmaco Chimico Tecnologico
Università degli Studi di Siena, Via A. Moro, 53100 Siena (Italy)

[c] *Dr. I. Filippi, Dr. A. Naldini, Dr. G. Scalia, Prof. Dr. F. Carraro*
Dipartimento di Fisiologia
Università degli Studi di Siena, Via A. Moro, 53100 Siena (Italy)

[d] *Dr. E. Crespan, Dr. G. Maga*
Istituto di Genetica Molecolare IGM-CNR
Via Abbiategrasso 207, 27100 Pavia (Italy)

Supporting information for this article is available on the WWW under http://dx.doi.org/10.1002/cmdc.201100304.

velopment of second-generation small-molecule inhibitors that are able to treat imatinib-resistant CML.[6]

We considered the importance of the (phenyl)pyrimidine-2-amine scaffold in the inhibition of Bcr-Abl,[7] and we focused our attention on the possibility of substituting the amide bond present in the structure of imatinib with a 1,2,3-triazole ring.[8] The bioisosterism between an amide group and a 1,2,3-triazole ring is well known[9] and is supported by docking simulations. Herein we report the versatile synthesis, biological evaluation, and modeling studies of a small collection of triazole-based imatinib analogues. To the best of our knowledge, this is the first time that the amide bond of any kinase inhibitor has been substituted by a triazole ring.

Results and Discussion

Chemistry

All the compounds were obtained by copper(I)-catalyzed azide–alkyne cycloaddition (CuAAC) according to Sharpless conditions,[10] between azides **6** and five different alkynes. The azides were synthesized as shown in Scheme 1, by using a route that partially follows the reported preparation of imatinib.[11]

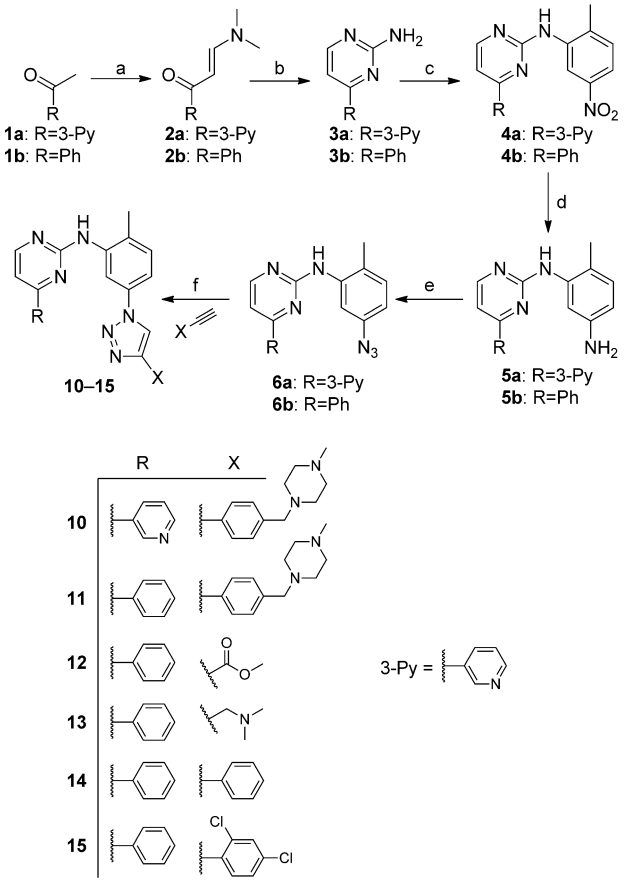

Scheme 1. *Reagents and conditions*: a) DMF-DMA, xylene; b) $C(NH_2)_3NO_3$, NaOH, *n*BuOH; c) *o*-Bromo-*p*-nitrotoluene, CuI, DMEDA, dioxane; d) N_2H_4, $FeCl_3$, active C, MeOH; e) $NaNO_2$, H_2SO_4, NaN_3, H_2O; f) sodium ascorbate, $CuSO_4 \cdot 5H_2O$, *t*BuOH/H_2O = 1:1. See the Experimental for reaction temperatures and times.

The reaction of 3-acetylpyridine **1a** and acetophenone **1b** with excess dimethylformamide dimethyl acetal (DMF-DMA) in xylene gave the corresponding enaminones **2a**–**b**. Compounds **2** reacted with guanidine nitrate and sodium hydroxide in *n*-butanol, with subsequent formation of the pyrimidine ring, leading to compounds **3a**–**b**. The third step consists of an "Ullmann-type" coupling between **3** and *o*-bromo-*p*-nitrotoluene. This reaction was performed in the presence of copper iodide, *N*,*N*′-dimethylethane-1,2-diamine (DMEDA), and potassium carbonate in dioxane at reflux to furnish nitro derivatives **4a**–**b**. The reduction of the nitro group with hydrazine monohydrate/iron(III) chloride in the presence of active carbon gave the corresponding amines **5a**–**b**.

The production of the azide derivative was secured by the formation of diazonium salt and subsequent reaction with a solution of sodium azide in water, leading to the key intermediates **6a**–**b**. The reaction of **6** with various alkynes in the presence of copper(II) sulfate pentahydrate and sodium ascorbate gave the corresponding 1–4 adducts **10**–**15** (6–76% yield). Alkyne **8** is the one that contains the 1-benzyl-4-methylpiperazine framework, which characterizes imatinib. The other four alkynes were selected to evaluate the efficacy of the CuAAC reaction with various types of alkyne and the relevance of the piperazine ring to biological activity. Three of the alkynes used are commercially available: methyl propiolate, 3-dimethylamino-1-propyne, and phenylacetylene, whereas the remaining two—4-methylpiperazine derivative **8** and 2,4-dichloroethynylbenzene **9**—were prepared with 4-ethynylbenzaldehyde and 2,4-dichlorobenzaldehyde as starting materials (Schemes 2 and 3). 4-Ethynylbenzaldehyde was reduced with

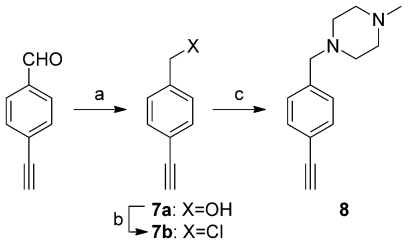

Scheme 2. *Reagents and conditions*: a) $NaBH_4$, MeOH, −78 °C, 30 min; b) $SOCl_2$, CH_2Cl_2, 60 °C, 4 h; c) *N*-methylpiperazine, 140 °C, 40 min.

sodium borohydride to the corresponding benzyl alcohol **7a**, which, by reaction with excess thionyl chloride, gave the chloro derivative **7b**. Treatment with *N*-methylpiperazine at reflux gave alkyne **8**. Alkyne **9** was obtained by homologation of 2,4-dichlorobenzaldehyde under Bestmann–Ohira conditions (Scheme 3).[12]

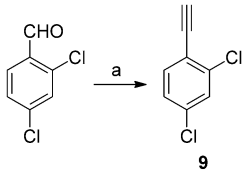

Scheme 3. a) Bestmann–Ohira reagent, K_2CO_3, MeOH, 0 °C, then RT, 20 h.

Biological evaluation

To assess the potency of our compounds, we evaluated their effects

on enzymatic activity, cell proliferation, phosphorylation, cdc25A expression, and pro-apoptotic activity. Imatinib was used as the reference compound.

Enzymatic activity

The compound FA030 was tested in an in vitro assay against the recombinant Abl kinase. It displayed potent anti-enzymatic activity, with an IC_{50} value of 0.9 ± 0.1 μM, while under our experimental conditions, imatinib showed a slightly lower IC_{50} value of 0.40 ± 0.1 μM. When tested against the imatinib-resistant mutant Abl T315I, however, FA030 activity was significantly lower, showing an IC_{50} value of 10 μM. None of the other compounds showed significant inhibitory activity toward Abl ($IC_{50} > 100$ μM). None of the tested compounds showed inhibitory activity against Src kinase up to a final concentration of 100 μM. FA030 was also tested against two additional tyrosine kinases: Hck and Pim1; the compound did not show significant inhibition up to 100 μM.

Inhibition of proliferation

The decrease in the viability of K-562, MEG-01, and KU-812 cells treated with the compounds for 72 h was assessed with the resazurin assay. Experiments performed to determine the in vitro effects of such compounds revealed the significant antiproliferative activity of FA030. In fact, activity data were in the low micromolar range (Table 1). No similarly good biological activity was observed among the other compounds. The biological profile in terms of activity toward Abl and cell lines encouraged the selection of FA030 (**10**) for further assays.

Inhibition of Bcr-Abl, c-Abl, STAT-5, and Src phosphorylation

With the aim of an improved understanding of the antiproliferative activity of this new compound toward leukemia cells, we decided to check, in each cell line, a direct link between the antiproliferative effects of FA030 and the inhibition of Bcr-Abl activity. Specifically, we evaluated the phosphorylation of Bcr-Abl, c-Abl, and its downstream substrate STAT-5, in K-562 and MEG-01 cells in addition to the phosphorylation of Src in KU-812 cells. Recent studies with Src dominant-negative mutants suggest that Src kinases play a role in proliferation of Bcr-Abl-expressing cell lines,[13] and overexpression of Src kinases is implicated in Bcr-Abl-mediated leukemogenesis and in imatinib resistance. As shown in Figure 2, after 3 h we observed a significant decrease in the phosphorylation of all targets in the presence of selected compounds relative to control. The dose-dependent inhibition of FA030 is similar to the effect of imatinib.

Table 1. Antiproliferative activity of compounds **10**–**15** against the indicated cell lines.

Compd	IC_{50} [μM][a]		
	K-562	MEG-01	KU-812
10 (FA030)	0.89 ± 0.003	10.97 ± 0.46	25.42 ± 1.24
11	56.45 ± 2.08	88.01 ± 2.05	>100
12	>100	>150	>150
13	24.22 ± 0.28	68.64 ± 0.9	77.36 ± 3.11
14	>100	>150	>150
15	>150	>150	>150
imatinib	0.37 ± 0.09	10.77 ± 0.41	1.89 ± 0.14

[a] Values represent the mean ± SEM for separate assays ($n = 3$), each performed in triplicate.

Inhibition of cdc25A expression

Through the Ras pathways, Bcr-Abl controls the activity of cell division cycle 25 (cdc25).[14] Cdc25 phosphatases are key regulators of the cell cycle and its checkpoints. They are required to dephosphorylate, and thus activate, the Cdk–cyclin complexes that trigger progression through the various cell-cycle phases. Cdc25A is required for the progression from G_1 to the S phase and G_2M in the cell cycle, and has been shown to be overexpressed in a number of cancer cells.[15] For this reason, we examined the action of FA030 on cdc25A expression. Figure 3 shows that this compound significantly inhibited cdc25A mRNA levels after 3 h in K-562 cells, and this inhibition was increased after 24 h exposure in the K-562 line (panel A). A similar inhibitory effect at 24 h exposure was also observed in MEG-01 cells (panel B). Notably, FA030 was observed to be more active at 24 h than imatinib in the inhibitory effect, toward both cell lines, even if these differences are not significant. This may be due to a direct effect of FA030 on the Ras Raf1 pathways.

Pro-apoptotic activity: PARP assay and studies on Bax/Bcl-xL expression

The new compound was also evaluated for its ability to induce apoptosis in the human leukemia cell line incubated for 72 h at the same concentration (1 μM) of the reference compound (imatinib). First, we investigated the expression of pro-apoptotic Bax and anti-apoptotic Bcl-xL genes, and we monitored the ratio between Bax and Bcl-xl mRNA expression as a direct indicator of the induction of apoptosis at the gene level. As a result, incubation of cells for 24 h in the presence of FA030 or imatinib led to an increase in the Bax/Bcl-xL ratio (Figure 4 A,C) in K-562 and MEG-01 cells. The same results were obtained in KU-812 cells, but this effect was already present after a 3 h incubation (Figure 4 E). Finally, on the basis of the ability of this compound to induce an increase in the ratio of the pro-apoptotic versus anti-apoptotic genes in both cell lines, we also evaluated the induction of caspase activity on the cleavage of Poly(ADP-ribose) polymerase (PARP) after incubation for 72 h. FA030 as well as imatinib potently induced apoptosis in K-562, MEG-01, and KU-812 cells, as shown by the presence of the cleaved form of PARP in immunoblots (Figure 4 B,D,F).

Molecular modeling

To better elucidate the structure–activity relationships (SAR), all compounds, after protocol validation (see the Experimental

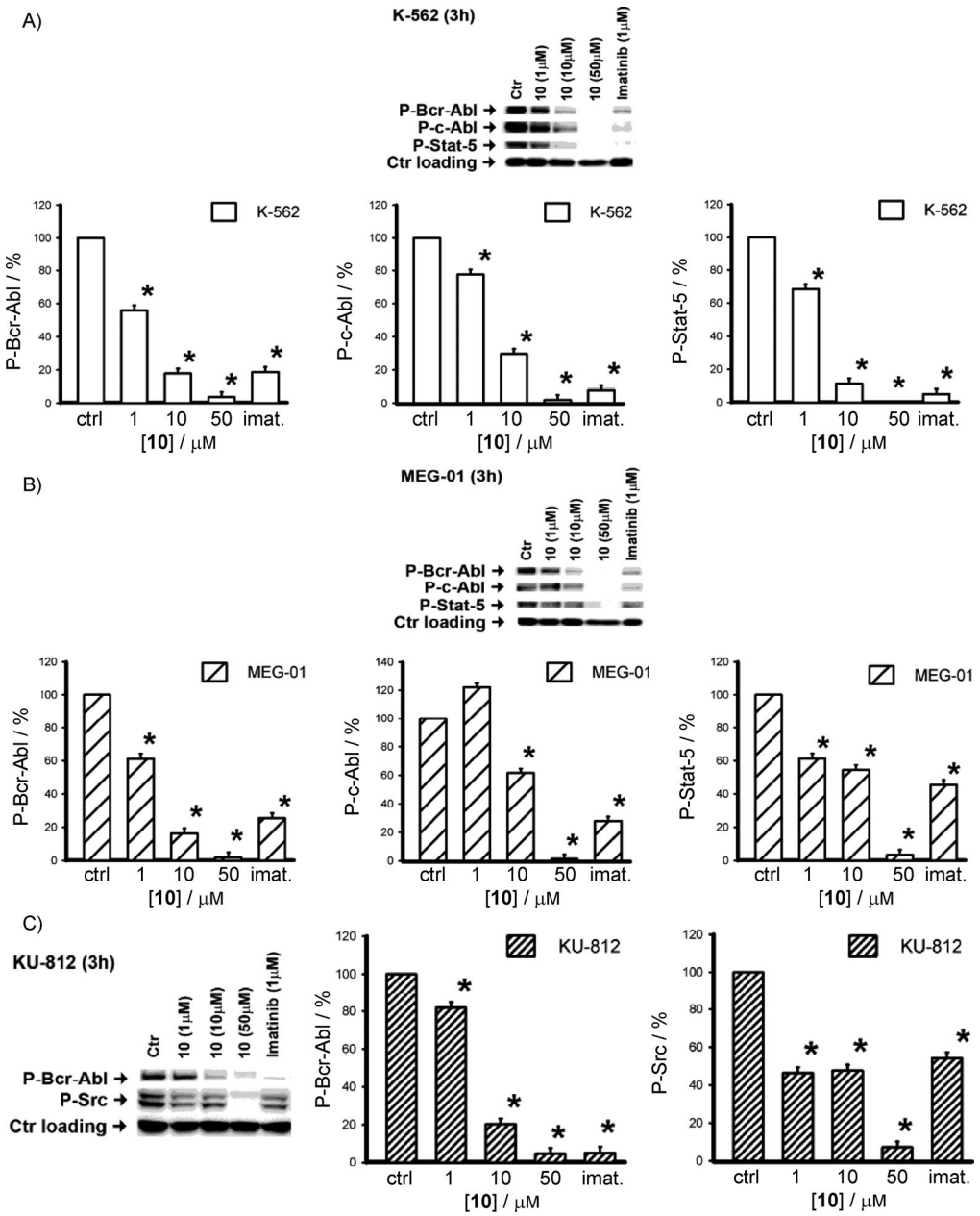

Figure 2. FA030 at various concentrations decreases phosphorylation of Bcr-Abl, c-Abl, and STAT-5 in A) K-562 and B) MEG-01 cells incubated for 3 h, with imatinib used as reference compound. FA030 also decreases phosphorylation of Bcr-Abl and Src in C) KU-812 cells. Data were quantified by chemiluminescence, and are expressed as percent phosphorylated protein. Statistical significance: $*p < 0.05$ (Student's *t* test).

Section below), were docked into the imatinib binding site of Abl kinase in the inactive conformation. We selected the inactive conformation of Abl because our compounds are strictly similar, in terms of functionality and shape, to imatinib, which binds to the inactive conformation.[16] For all compounds, the binding mode is very similar to that of imatinib (Figure 5). Compound **10** (FA030) seems to have six hydrogen bonds with the protein, and the majority of contacts are mediated by van der Waals interactions. Hydrogen bond interactions are predicted between the pyridine nitrogen atom and the backbone NH group of Met 318 in the hinge region, and the anilino NH group with the side chain of the gatekeeper residue Thr 315. In comparison with imatinib, FA030 loses a hydrogen bond with the backbone NH group of Ala 380, but two hydrogen bonds between the triazole ring and the side chain of Asp 381 are allowed. The *N*-methylpiperazine group is predicted to have a strong interaction with the protein by hydrogen bonds with the main-chain carbonyl groups of Asp 381 and His 361, whereas imatinib interacts with the main-chain carbonyl groups of Ile 360 and His 361. The difference is most likely due to the small difference in length between FA030 and imatinib. These hydrogen bonds are complemented by extensive hydrophobic interactions (Val 256, Tyr 253, Leu 248, Leu 370, Phe 317, Phe 382, Gly 321, Lys 271, Thr 315, Ile 313, Val 289,

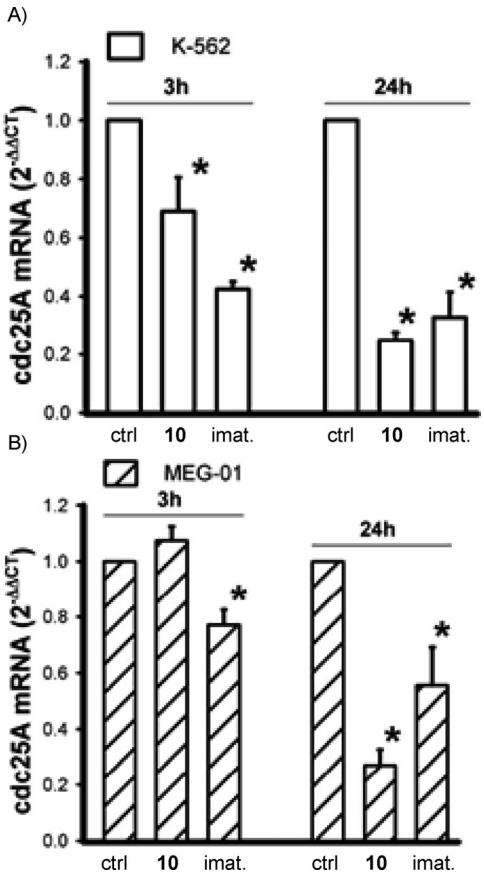

Figure 3. FA030 inhibits cdc25A expression at 3 and 24 h in A) K-562 and B) MEG-01 cells, with imatinib used as reference compound; both compounds were used at 1 μM. The results were obtained by qRT-PCR analysis. Statistical significance: $*p < 0.05$ (Student's *t* test).

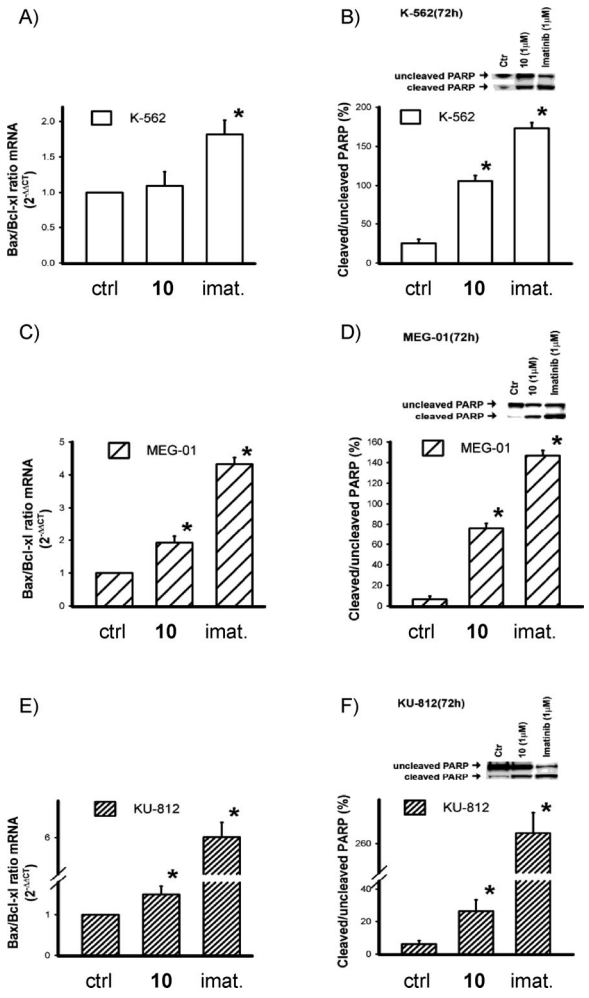

Figure 4. Pro-apoptotic effect of FA030 relative to imatinib used at the same concentration (1 μM). The ratio of Bax/Bcl-xL mRNA expression at 24 h in A) K-562 and C) MEG-01 cells, and at 3 h in E) KU-812 cells was determined by qRT-PCR. PARP cleavage at 72 h in B) K-562, D) MEG-01, and F) KU-812 cells was analyzed by immunoblots, and two forms of PARP were quantified by chemiluminescence; results are expressed as the percentage of cleaved over uncleaved PARP. Statistical significance: $*p < 0.05$ (Student's *t* test).

Met 290, and Asp 381) over the whole length of the inhibitor, although there are fewer hydrophobic interactions for the *N*-methylpiperazine, which is partially exposed to water. For all remaining compounds, the binding mode is similar to that of FA030 apart from the hydrogen bond with the hinge region (the nitrogen atom of pyridine is missing). Concerning the docking score, FA030 has a value similar to that of imatinib (−12.7 versus −13.7), and all this confirms the good protein affinity. For all the other molecules, there is a significant loss in score (values range from −7.0 to −8.4). This is due to the loss of the hydrogen bond with the hinge region. Structures **12** and **13**, in addition to this lost hydrogen bond, also set up polar groups in the hydrophobic region.

Regarding the T315I mutation, FA030 (with a very similar shape to that of imatinib) undergoes the same problems of steric hindrance and loss of a hydrogen bond[17] when Tyr 315 is replaced by Ile 315, thus diminishing its activity (10 μM for T315I versus 0.9 μM for wild-type).

Finally, from the ADME point of view (calculated with QikProp), there is no significant difference between imatinib and FA030. All the other compounds give similar properties to FA030, except for **14** and **15**, which have poor solubility (see the Supporting Information for details).

Conclusions

Herein we have described the design and preparation of a small collection of *N*-[2-methyl-5-(triazol-1-yl)phenyl]pyrimidin-2-amine derivatives using a copper(I)-catalyzed azide–alkyne cycloaddition. Preliminary antiproliferative activity in the micromolar range highlighted the efficacy of compound **10** (FA030). This compound shows potent anti-enzymatic activity against recombinant Abl kinase, but decreased activity against the imatinib-resistant mutant Abl T3151. FA030 is able to decrease the phosphorylation of Bcr-Abl, c-Abl, STAT-5, and Src with a dose-dependent behavior similar to the effect observed for imatinib; in addition, FA030 is more active than imatinib in the inhibition of cdc25A in two different cell lines. The pro-apoptotic activity of FA030 has been proven by the presence of the cleaved form of PARP, after treatment of three different cell lines. The ADME prediction suggests no significant difference from the behavior of imatinib. Molecular modeling studies pre-

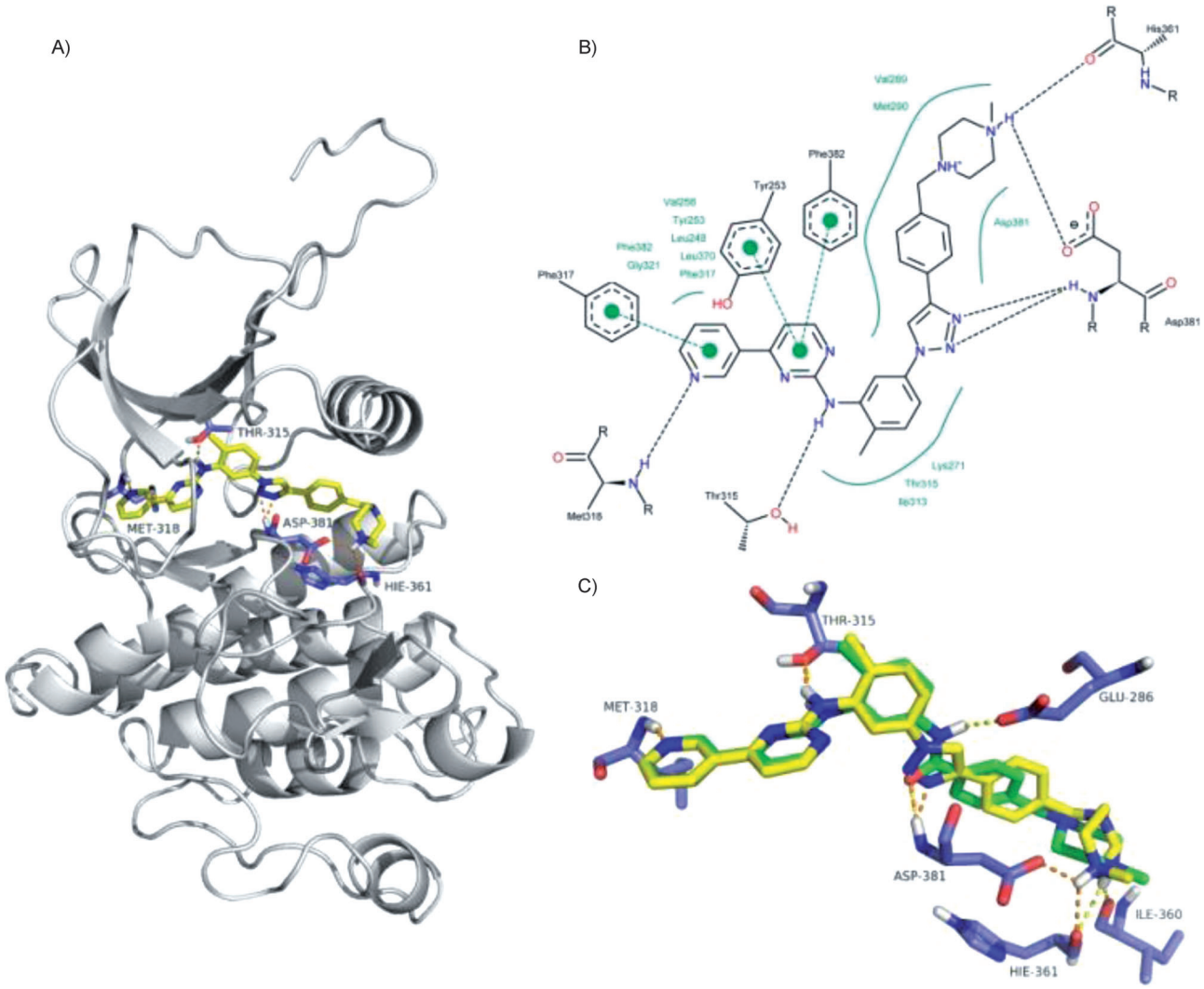

Figure 5. A) Ribbon representation of the Abl kinase domain (grey) in complex with FA030 (yellow). B) Schematic diagram of the interactions made by FA030 with Abl (from docking calculations); protein residues are labeled, and hydrogen bonds are indicated with dotted lines; residues making van der Waals interactions with the inhibitor are shown in green. C) Comparison of the binding modes of FA030 (yellow) and imatinib (green).

dict a similar binding mode to that of imatinib, with some slightly different interactions.

Experimental Section

Chemistry

General. Thin-layer chromatography (TLC) was performed with Merck pre-coated 60 F_{254} plates. Reactions were monitored by TLC on silica gel, with detection by UV light (λ 254 nm). Flash chromatography was performed using silica gel (240–400 mesh, Merck). ^{1}H NMR spectra were recorded with Bruker 300 and 400 MHz spectrometers using $CDCl_3$ and [D_6]DMSO. Chemical shifts (δ) are reported in ppm downfield from $(CH_3)_4Si$ as an internal standard. EI mass spectra were recorded at an ionizing voltage of 6 keV on a VG 70–70 EQ instrument. ESI mass spectra were recorded on an FT-ICR APEX^{II} instrument (Bruker Daltonics).

(*E*)-3-(Dimethylamino)-1-(pyridine-3-yl)prop-2-en-1-one (2a).[10] A solution of 4-acetylpyridine (50 mmol) and *N*,*N*-dimethylformamide dimethylacetal (100 mmol) in xylene (50 mL) was held at reflux at 140 °C for 20 h. The solvent was removed in vacuo, and hexane (200 mL) was added, with consequent formation of yellow crystals. After complete crystallization, the product was collected by filtration in 81% yield. No further purification was needed. ^{1}H NMR ($CDCl_3$, 300 MHz): δ = 9.02 (1H, s), 8.61 (1H, dd, J = 5.3, 2.7 Hz), 8.15 (1H, dd, J = 8.0 Hz, J = 2.7 Hz), 7.80 (1H, d, J = 12 Hz), 7.31 (1H, dd, J = 8.0 Hz, J = 5.3 Hz), 5.67 (1H, d), 3.16 (3H, s), 2.94 ppm (3H, s).

(*E*)-3-(Dimethylamino)-1-phenylprop-2-en-1-one (2b).[10] A solution of acetophenone (25 mmol) and *N*,*N*-dimethylformamide dimethylacetal (100 mmol) xylene (50 mL) was held at reflux at 180 °C for 11 h. The solvent was removed in vacuo and hexane (200 mL) was added, with consequent formation of yellow crystals. After complete crystallization, the product was collected by filtration in 32% yield. No further purification was needed. ^{1}H NMR ($CDCl_3$, 300 MHz): δ = 7.88 (2H, d, J = 6.3 Hz), 7.79 (1H, d, J = 12.4 Hz), 7.46–7.36 (3H, m), 3.14 (3H, bs), 2.92 ppm (3H, bs).

4-(Pyridine-3-yl)pyrimidin-2-amine (3a).[10] $C(NH_2)_3NO_3$ (40.3 mmol) and NaOH (40.3 mmol) were added to a solution of **2a** (40.3 mmol) in *n*BuOH (45 mL). The reaction mixture was held at

reflux at 120 °C for 4 h, then cooled to room temperature. The precipitate was collected by filtration and washed with H_2O (70 mL), then dried in the oven at 75–80 °C. No further purification was needed, and the desired product was obtained as white crystals in 60% yield. ^{1}H NMR ($CDCl_3$, 300 MHz): δ = 9.21 (1H, d, J = 2.6 Hz), 8.63 (1H, d, J = 3.3 Hz), 8.47 (1H, dt, J = 8.3 Hz, J = 1.7 Hz), 8.33 (1H, d, J = 5.9 Hz), 7.55 (1H, dd, J = 8.3 Hz, J = 3.3 Hz), 7.19 (1H, d, J = 5.9 Hz), 4.86 ppm (1H, s).

4-Phenylpyrimidin-2-amine (3b).[10] $C(NH_2)_3NO_3$ (7.1 mmol) and NaOH (7.1 mmol) were added to a solution of **2b** (7.1 mmol) in *n*BuOH (70 mL). The reaction mixture was held at reflux at 130 °C for 15 h, then cooled to room temperature. The precipitate was collected by filtration, washed with H_2O (70 mL) and dried in the oven at 75–80 °C. No further purification was needed, and the desired product was obtained as white crystals in 49% yield. ^{1}H NMR ($CDCl_3$, 300 MHz): δ = 8.30 (1H, d, J = 5.6 Hz), 8.00–7.97 (2H, m), 7.48–7.46 (3H, m), 7.04 (1H, d, J = 5.6 Hz), 5.27 ppm (2H, bs).

***N*-(2-Methyl-5-nitrophenyl)-4-(pyridin-3-yl)pyrimidin-2-amine (4a).**[10] *o*-Bromo-*p*-nitrotoluene (1.0 mmol), CuI (0.25 mmol), DMEDA (0.25 mmol), and K_2CO_3 (2.0 mmol) were added to a solution of **3a** (1.1 mmol) in dry dioxane (5 mL) under N_2 atmosphere, and the reaction mixture was held at reflux at 120 °C for 15 h, then cooled to room temperature. Concentrated NH_3 (4 mL) and brine (20 mL) were added, and extracted with EtOAc. The organic layers were dried over Na_2SO_4 and concentrated in vacuo. The crude was purified by column chromatography on silica gel (MeOH/CH_2Cl_2 = 1:80) to give the desired product as a pale-yellow powder in 40% yield. ^{1}H NMR ($CDCl_3$, 300 MHz): δ = 9.47 (1H, d, J = 1.8 Hz), 9.28 (1H, bs), 8.76 (1H, d, J = 4.3 Hz), 8.59 (1H, d, J = 6.5 Hz), 7.87 (1H, dd, J = 7.2 Hz, J = 1.8 Hz), 7.54 (1H, dd, J = 7.2 Hz, J = 4.3 Hz), 7.38 (1H, s), 7.32 (1H, d, J = 6.5 Hz), 7.23 (1H, bs), 2.44 ppm (3H, s); ^{13}C NMR ($CDCl_3$, 100 MHz): δ = 159.32, 158.76, 147.19, 146.94, 144.44, 139.02, 137.65, 134.58, 132.09, 131.03, 125.68, 118.14, 115.48, 109.03, 29.71, 18.42 ppm.

***N*-(2-Methyl-5-nitrophenyl)-4-phenylpyrimidin-2-amine (4b)**.[10] *o*-Bromo-*p*-nitrotoluene (4.7 mmol), CuI (1.3 mmol), DMEDA (1.3 mmol), and K_2CO_3 (10.5 mmol) were added to a solution of **3b** (5.2 mmol) in dry dioxane (23 mL) under N_2 atmosphere, and the reaction mixture was held at reflux at 120 °C for 15 h, then cooled to room temperature. Concentrated NH_3 (12 mL) and brine (60 mL) were added and extracted with EtOAc. The organic layers were dried over Na_2SO_4 and concentrated in vacuo. The crude was purified by column chromatography on silica gel (EtOAc/hexane = 1:1) to give the desired product as pale-yellow powder in 31% yield. ^{1}H NMR ([D_6]DMSO, 300 MHz): δ = 9.16 (1H, s), 8.89 (1H, d, J = 2.6 Hz), 8.60 (1H, d, J = 5.0 Hz), 8.20–8.17 (2H, m), 7.92–7.89 (1H, m), 7.56–7.51 (5H, m), 4.46 ppm (3H, s).

6-Methyl-*N*-[4-(pyridine-3-yl)pyrimidin-2-yl]benzene-1,3-diamine (5a).[10] $H_2NNH_2{\cdot}H_2O$ (3.91 mmol), $FeCl_3$ (0.02 mmol), and active carbon (0.001 g) were added to a solution of **4a** (0.98 mmol) in MeOH (10 mL), and the reaction mixture was held at reflux at 80 °C for 6 h. The solvent was removed in vacuo, H_2O (30 mL) was added, and extracted with CH_2Cl_2 (3×10 mL). The organic layers were dried over Na_2SO_4 and concentrated in vacuo. No further purification was needed, and the desired product was collected as a yellow powder in 99% yield. ^{1}H NMR ([D_6]DMSO, 300 MHz): δ = 9.22 (1H, s), 8.67 (1H, d, J = 4.4 Hz), 8.63 (1H, s), 8.44 (1H, d, J = 5.1 Hz), 8.39 (1H, d, J = 8.0 Hz), 7.51 (1H, dd, J = 7.9, 4.4 Hz), 6.85 (1H, d, J = 8.0 Hz), 6.77 (1H, d, J = 1.4 Hz), 6.32 (1H, dd, J = 8.0, 2.0 Hz), 4.80 (2H, s), 2.04 ppm (3H, s); ^{13}C NMR ([D_6]DMSO, 100 MHz): δ = 168.6, 161.1, 154.4, 147.9, 147.8, 147.5, 144.8, 134.0, 133.0, 130.6, 124.0, 119.0, 105.1, 103.3, 102.6, 17.6 ppm.

6-Methyl-*N*-(4-phenylpyrimidin-2-yl)benzene-1,3-diamine (5b).[10] $H_2NNH_2{\cdot}H_2O$ (25.6 mmol), $FeCl_3$ (0.03 mmol), and active carbon (0.010 g) were added to a solution of **4b** (1.6 mmol) in MeOH (20 mL), and the reaction mixture was held at reflux at 100 °C for 4 h. The solvent was removed in vacuo, H_2O (100 mL) was added, and extracted with CH_2Cl_2 (3×30 mL). The organic layers were dried over Na_2SO_4 and concentrated in vacuo. No further purification was needed, and the desired product was collected as a yellow powder in 93% yield. ^{1}H NMR ($CDCl_3$, 300 MHz): δ = 8.41 (1H, d, J = 5.0 Hz), 8.06–8.02 (2H, m), 7.65 (1H, d, J = 2.3 Hz), 7.52–7.48 (3H, m), 7.41 (1H, bs), 7.14 (1H, d, J = 5.8 Hz), 7.00 (1H, d, J = 8.0 Hz), 6.46 (1H, dd, J = 7.9 Hz, J = 2.1 Hz), 4.0–3.1 (2H, bs), 2.26 ppm (3H, s).

***N*-(5-Azido-2-methylphenyl)-4-(pyridine-3-yl)pyrimidin-2-amine (6a).** Compound **5a** (0.292 g, 1.06 mmol) was suspended in H_2O (15 mL) and was cooled to 0 °C, then concentrated H_2SO_4 was added until **5a** was completely dissolved. A solution of $NaNO_2$ (1.59 mmol) in H_2O (2 mL) was added, and the reaction mixture was stirred at 0 °C for 30 min. Then a solution of NaN_3 (2.12 mmol) in H_2O (2 mL) was added at 0 °C, and the reaction mixture was stirred at room temperature for 3 h. K_2CO_3 was added until the solution reached pH 8, and the reaction mixture was extracted with CH_2Cl_2. The organic layers were dried over Na_2SO_4 and concentrated in vacuo. No further purification was needed, and the desired product was collected as an orange amorphous solid in 81% yield. ^{1}H NMR ($CDCl_3$, 400 MHz): δ = 9.26 (1H, bs), 8.74 (1H, d, J = 3.4 Hz), 8.53 (1H, d, J = 5.1 Hz), 8.42 (1H, d, J = 7.8 Hz), 8.21 (1H, d, J = 2.1 Hz), 7.46 (1H, dd, J = 7.9 Hz, J = 7.8 Hz), 7.22 (1H, d, J = 5.1 Hz), 7.16–7.19 (2H, m), 6.68 (1H, dd, J = 8.1 Hz, J = 2.1 Hz), 2.34 ppm (3H, s); ^{13}C NMR ($CDCl_3$, 100 MHz): δ = 163.32, 160.99, 159.71, 152.20, 149.07, 139.38, 139.13, 135.25, 133.23, 132.03, 124.36, 114.29, 111.62, 109.28, 30.32, 18.13 ppm; Anal. calcd for $C_{16}H_{13}N_7$: C 63.36, H 4.32, N 32.32, found: C 63.41, H 4.29, N 32.35.

***N*-(5-Azido-2-methylphenyl)-4-phenylpyrimidin-2-amine (6b)**. Compound **5b** (1.5 mmol) was suspended in H_2O (70 mL) and cooled to 0 °C, then concentrated H_2SO_4 was added until **5b** was completely dissolved. A solution of $NaNO_2$ (2.2 mmol) in H_2O (9 mL) was added and the reaction mixture was stirred at 0 °C for 30 min. Then a solution of NaN_3 (2.9 mmol) in H_2O (9 mL) was added at 0 °C, and the reaction mixture was stirred at room temperature for 3 h. K_2CO_3 was added until the solution reached pH 8, and the reaction mixture was extracted with CH_2Cl_2 (4×30 mL). The organic layers were dried over Na_2SO_4 and concentrated in vacuo. No further purification was needed, and the desired product was collected as an orange amorphous solid in 92% yield. ^{1}H NMR ($CDCl_3$, 300 MHz): δ = 8.46 (2H, d, J = 5.2 Hz), 8.32 (1H, d, J = 2.1 Hz), 8.10–8.05 (2H, m), 7.51–7.49 (2H, m), 7.21–7.13 (3H, m), 6.64 (1H, dd, J = 7.9 Hz, J = 2.7 Hz), 2.33 ppm (3H, s); Anal. calcd for $C_{17}H_{14}N_6$: C 67.54, H 4.67, N 27.80, found: C 67.51, H 4.69, N 27.77.

(4-Ethynylphenyl) methanol (7a). A solution of 4-ethynylbenzaldehyde (1.5 mmol) in MeOH (10 mL) was cooled to −78 °C, and $NaBH_4$ (0.4 mmol) was added in small amounts. The reaction mixture was stirred at −78 °C for 30 min and then warmed to room temperature. HCl (1 N) was added to quench unreacted $NaBH_4$, and the solvent was removed in vacuo. H_2O (50 mL) was added and extracted with EtOAc (3×15 mL). The organic layers were dried over Na_2SO_4 and concentrated in vacuo. The crude was purified by column chromatography on silica gel (EtOAc/hexane = 3:7), and the desired product was obtained as a white amorphous solid in

44% yield. ^{1}H NMR ($CDCl_3$, 300 MHz): δ = 7.47 (2H, d, J = 8.4 Hz), 7.33 (2H, d, J = 8.4 Hz), 4.57 (2H, s), 3.09 ppm (1H, s); ^{13}C NMR ($CDCl_3$, 100 MHz): δ = 141.6, 131.1 (2C), 126.9 (2C), 121.8, 83.6, 81.9, 64.1 ppm; Anal. calcd for C_9H_8O: C 93.06, H 6.94, found: C 93.12, H 7.01.

4-Ethynyl chloromethylbenzene (7b). $SOCl_2$ (2 mL) was added to a solution of **7a** (0.7 mmol) in CH_2Cl_2 (2 mL), and the reaction mixture was held at reflux at 60 °C for 4 h. Then the volatiles were removed in vacuo, and the crude was purified by column chromatography on silica gel (Hex). The desired product was obtained as pale-yellow oil in 47% yield. ^{1}H NMR ($CDCl_3$, 300 MHz): δ = 7.47 (2H, d, J = 8.4 Hz), 7.33 (2H, d, J = 8.4 Hz), 4.57 (2H, s), 3.09 ppm (1H, s); ^{13}C NMR ($CDCl_3$, 100 MHz): δ = 138.1, 132.2 (2C), 128.9 (2C), 123.4, 81.8, 80.9, 47.5 ppm; Anal. calcd for C_9H_7Cl: C 71.78, H 4.68, found: C 71.81, H 4.65.

1-(4-Ethynylbenzyl)-4-methylpiperazine (8). A solution of **7b** (0.3 mmol) and *N*-methylpiperazine was held at reflux at 140 °C for 40 min. H_2O (30 mL) was added and extracted with CH_2Cl_2 (3× 10 mL). The organic layers were dried over Na_2SO_4 and concentrated in vacuo. The crude was purified by column chromatography on silica gel (CH_2Cl_2/MeOH = 20:1), and the desired product was obtained as a colorless oil in 75% yield. ^{1}H NMR ($CDCl_3$, 300 MHz): δ = 7.42 (2H, d, J = 8.3 Hz), 7.26 (2H, d, J = 8.3 Hz), 3.49 (2H, s), 3.04 (1H, s), 2.49 (8H, bs), 2.31 ppm (3H, s); ^{13}C NMR ($CDCl_3$, 100 MHz): δ = 138.8, 132.5 (2C), 127.9 (2C), 121.1, 85.5, 81.9, 63.7, 56.9 (2C), 54.1 (2C), 46.7 ppm; Anal. calcd for $C_{14}H_{18}N_2$: C 78.46, H 8.47, N 13.07, found: C 78.49, H 8.41, N 13.12.

2,4-Dichloro-ethynylbenzene (9). A solution of 2,4-dichlorobenzaldehyde (0.6 mmol) in dry MeOH (20 mL) was cooled to 0 °C and then K_2CO_3 (1.2 mmol) and dimethyl-1-diazo-2-oxopropylphosphonate (0.7 mmol) were added. The reaction mixture was stirred at room temperature for 20 h. The solvent was removed in vacuo, saturated $NaHCO_3$ (70 mL) was added, and extracted with EtOAc (3× 20 mL). The organic layers were dried over Na_2SO_4 and the solvent was removed in vacuo. The crude was purified by column chromatography on silica gel (EtOAc/hexane = 1:1) and the desired product was obtained as a white amorphous solid in 41% yield. ^{1}H NMR ($CDCl_3$, 300 MHz): δ = 7.46–7.42 (2H, m), 7.20 (1H, dd, J = 8.6 Hz, J = 1.7 Hz), 3.39 ppm (1H, s); ^{13}C NMR ($CDCl_3$, 100 MHz): δ = 136.8, 135.3, 135.0, 129.8, 127.0, 115.8, 83.1, 81.2 ppm; Anal. calcd for $C_8H_4Cl_2$: C 56.18, H 2.36, found: C 56.23, H 2.31.

***N*-[2-Methyl-5-(4-{4-[(4-methylpiperazin-1-yl)methyl]phenyl}-1*H*-1,2,3-triazol-1-yl)phenyl]-4-(pyridine-3-yl)pyrimidin-2-amine (10).** Sodium ascorbate (0.02 mmol) and $CuSO_4{\cdot}5H_2O$ (0.001 g) were added to a solution of **6a** (0.23 mmol) and **8** (0.23 mmol) in H_2O/*t*BuOH = 1:1 (5 mL), and the reaction mixture was stirred at room temperature for 24 h. The reaction mixture was filtered and the solid was washed with H_2O and dried in the oven at 80 °C. The crude was purified by column chromatography on silica gel (MeOH/CH_2Cl_2 = 1:10) and the desired product was obtained as a yellow amorphous solid in 76% yield. ^{1}H NMR ($CDCl_3$, 400 MHz): δ = 9.32 (1H, bs), 9.05 (1H, bs), 8.77 (1H, bs), 8.59 (1H, d, J = 5.0 Hz), 8.53 (1H, d, J = 7.9 Hz), 8.22 (1H, s), 7.90 (2H, d, J = 7.8 Hz), 7.51 (1H, t, J = 7.9 Hz), 7.43–7.45 (3H, m), 7.37–7.39 (1H, d, J = 8.2 Hz), 7.28- 7.29 (2H, m), 3.59 (2H, s), 2.60 (8H, bs), 2.47 (3H, s), 2.38 ppm (3H, s); ^{13}C NMR ($CDCl_3$, 100 MHz): δ = 163.44, 160.94, 159.84, 152.41, 149.16, 148.80, 139.43, 138.94, 136.48, 135.32, 133.19, 131.94, 130.27 (2C), 130.08, 127.86, 126.49 (2C), 124.48, 118.07, 115.00, 113.14, 109.58, 63.22, 55.61 (2C), 53.22 (2C), 46.25, 18.34 ppm; Anal. calcd for $C_{30}H_{31}N_9$: C 69.61, H 6.04, N 24.35, found: C 69.65, H 6.10, N 24.31; MS (EI): m/z 517 $[M]^+$.

***N*-[2-Methyl-5-(4-{4-[(4-methylpiperazin-1-yl)methyl]phenyl}-1*H*-1,2,3-triazol-1-yl)phenyl]-4-phenylpyrimidin-2-amine (11).** Sodium ascorbate (0.007 mmol) and $CuSO_4{\cdot}5H_2O$ (0.001 g) were added to a solution of **6b** (0.07 mmol) and **8** (0.07 mmol) in H_2O/*t*BuOH = 1:1 (2.5 mL), and the reaction mixture was stirred at 80 °C for 1.5 h. The solvent was removed in vacuo, H_2O (10 mL) and brine (10 mL) were added, and extracted with CH_2Cl_2 (5×5 mL). The organic layers were dried over Na_2SO_4 and concentrated in vacuo. The crude was purified by column chromatography on silica gel (EtOAc/hexane = 1:2) and the desired product was obtained as a yellow amorphous solid in 6% yield. ^{1}H NMR ($CDCl_3$, 300 MHz): δ = 9.08 (1H, d, J = 2.0 Hz), 8.54 (1H, bs), 8.21 (1H, s), 8.12–8.15 (2H, m), 7.85 (2H, d, J = 7.8 Hz), 7.51–7.53 (3H, m), 7.34–7.48 (5H, m), 7.16 (1H, bs), 3.63 (2H, s), 2.77 (8H, bs), 2.56 (3H, s), 2.44 ppm (3H, s); ^{13}C NMR ($CDCl_3$, 100 MHz): δ = 164.87, 163.10, 157.25, 154.37, 150.22, 149.19, 142.89, 139.06, 137.54, 136.21, 135.01, 132.74, 131.89 (2C), 131.65 (2C), 129.01, 127.99 (2C), 124.80, 119.45, 116.51, 114.87, 109.12, 64.38, 56.39 (2C), 55.03 (2C), 46.12, 17.90 ppm; Anal. calcd for $C_{31}H_{32}N_8$: C 72.07, H 6.24, N 21.69, found: C 72.11, H 6.20, N 21.68.

Methyl 1-[4-methyl-3-(4-phenylpyrimidin-2-ylamino)phenyl]-1*H*-1,2,3-triazole-4-carboxylate (12). Sodium ascorbate (0.016 mmol) and $CuSO_4{\cdot}5H_2O$ (0.001 g) were added to a solution of **6b** (0.16 mmol) and methyl propiolate (0.16 mmol) in H_2O/*t*BuOH = 1:1 (3 mL), and the reaction mixture was stirred at 50 °C for 5 h. The solvent was removed in vacuo, H_2O (30 mL) was added and extracted with CH_2Cl_2 (4×10 mL). The organic layers were dried over Na_2SO_4 and concentrated in vacuo. The crude was purified by column chromatography on silica gel (EtOAc/hexane = 1:1) and the desired product was obtained as an orange amorphous solid in 41% yield. ^{1}H NMR ($CDCl_3$, 400 MHz): δ = 9.14 (1H, bs), 8.58 (1H, s), 8.51 (1H, d, J = 5.1 Hz), 8.13–8.15 (2H, m), 7.53–7.60 (3H, m), 7.40 (1H, dd, J = 8.3 Hz, J = 1.9 Hz), 7.36 (1H, d, J = 8.3 Hz), 7.31 (1H, bs), 7.26–7.28 (2H, m), 4.03 (3H, s), 2.46 ppm (3H, s); ^{13}C NMR ($CDCl_3$, 100 MHz): δ = 165.97, 161.83, 160.37, 159.03, 141.00, 139.80, 137.22, 135.68, 132.03, 131.90, 129.73(2C), 127.97, 127.85 (2C), 126.15, 114.71, 112.52, 109.82 ppm; Anal. calcd for $C_{21}H_{18}N_6O_2$: C 65.28, H 4.70, N 21.75, found: C 65.26, H 4.73, N 21.72; HRMS (EI): m/z $[M]^+$ calcd for $C_{21}H_{18}N_6O_2$: 386.1491, found: 386.1492.

***N*-[2-Methyl-5-{4-[(dimethylamino)methyl]-1*H*-1,2,3-triazol-1-yl}-phenyl]-4-phenylpyrimidin-2-amine (13).** Sodium ascorbate (0.016 mmol) and $CuSO_4{\cdot}5H_2O$ (0.001 g) were added to a solution of **6b** (0.16 mmol) and 3-dimethylamino-1-propyne (0.16 mmol) in H_2O/*t*BuOH = 1:1 (3 mL), and the reaction mixture was stirred at room temperature for 30 h. The solvent was removed in vacuo, H_2O (30 mL) was added and extracted with CH_2Cl_2 (4×10 mL). The organic layers were dried over Na_2SO_4 and concentrated in vacuo. No further purification was needed, and the desired product was obtained as a yellow amorphous solid in 16% yield. ^{1}H NMR ($CDCl_3$, 400 MHz): δ = 9.06 (1H, d, J = 1.8 Hz), 8.54 (1H, bs), 8.31 (1H, s), 8.13–8.15 (2H, m), 7.52–7.56 (3H, m), 7.39 (1H, dd, J = 8.2 Hz, J = 1.8 Hz), 7.34 (1H, d, J = 8.2 Hz), 7.25 (1H, d, J = 4.7 Hz), 7.18 (1H, bs), 3.99 (2H, bs), 2.55 (6H, bs), 2.45 ppm (3H, s); ^{13}C NMR ($CDCl_3$, 100 MHz): δ = 166.51, 164.12, 157.31, 145.64, 138.95, 136.28, 133.34, 131.13 (2C), 129.18, 128.95, 127.41 (2C), 126.82, 125.09, 119.87, 105.75, 99.28, 64.08, 49.25 (2C), 18.39 ppm; Anal. calcd for $C_{22}H_{23}N_7$: C 68.55, H 6.01, N 25.44, found: C 68.58, H 5.99, N 25.47; HRMS (EI): m/z $[M]^+$ calcd for $C_{22}H_{23}N_7$: 385.2015, found: 385.2005.

***N*-[2-Methyl-5-(4-phenyl-1*H*-1,2,3-triazol-1-yl)phenyl]-4-phenylpyrimidin-2-amine (14).** Sodium ascorbate (0.016 mmol) and $CuSO_4{\cdot}5H_2O$ (0.001 g) were added to a solution of **6b** (0.16 mmol)

and phenylacetylene (2.4 mmol) in H_2O/*t*BuOH = 1:1 (3.5 mL), and the reaction mixture was stirred at room temperature for 28 h. The solvent was removed in vacuo, H_2O (60 mL) was added and extracted with CH_2Cl_2 (4×20 mL). The organic layers were dried over Na_2SO_4 and concentrated in vacuo. The crude was purified by column chromatography on silica gel (EtOAc/hexane = 1:2) and the desired product was obtained as a yellow amorphous solid in 19% yield. ^{1}H NMR ($CDCl_3$, 400 MHz): δ = 9.10 (1H, d, J = 2.1 Hz), 8.53 (1H, d, J = 5.2 Hz), 8.25 (1H, s), 8.14–8.17 (2H, m), 7.92 (2H, dd, J = 8.4 Hz, J = 1.3 Hz), 7.53–7.56 (3H, m), 7.46–7.50 (3H, m), 7.36–7.41 (3H, m), 7.26 (1H, d, J = 5.2 Hz), 2.47 ppm (3H, s); ^{13}C NMR ($CDCl_3$, 100 MHz): δ = 166.04, 160.44, 158.90, 148.85, 139.52, 137.43, 136.40, 131.96, 131.83, 131.17, 129.70 (2C), 129.51 (2C), 128.94, 127.92 (2C), 127.52, 126.53 (2C), 118.25, 114.82, 112.64, 109.68, 18.46 ppm; Anal. calcd for $C_{25}H_{20}N_6$: C 74.24, H 4.98, N 20.78, found: C 74.26, H 5.02, N 20.75; HRMS (EI): *m/z* $[M]^+$ calcd for $C_{25}H_{20}N_6$: 404.1749, found: 404.1763.

***N*-[2-Methyl-5-(4-(2,4-dichlorophenyl)-1*H*-1,2,3-triazol-1-yl)phenyl]-4-phenylpyrimidin-2-amine (15).** Sodium ascorbate (0.016 mmol) and $CuSO_4 \cdot 5H_2O$ (0.001 g) were added to a solution of **6b** (0.16 mmol) and **9** (2.4 mmol) in H_2O/*t*BuOH = 1:1 (4 mL), and the reaction mixture was stirred at 70 °C for 6 h. The solvent was removed in vacuo, H_2O (50 mL) was added and extracted with CH_2Cl_2 (4×20 mL). The organic layers were dried over Na_2SO_4 and concentrated in vacuo. The crude was purified by column chromatography on silica gel (EtOAc/hexane = 2:3) and the desired product was obtained as a yellow amorphous solid in 44% yield. ^{1}H NMR ($CDCl_3$, 400 MHz): δ = 9.07 (1H, d, J = 2.1 Hz), 8.62 (1H, s), 8.53 (1H, d, J = 5.1 Hz), 8.33 (1H, d, J = 8.5 Hz), 8.14–8.16 (2H, m), 7.51–7.85 (4H, m), 7.45 (1H, dd, J = 8.1 Hz, J = 2.1 Hz), 7.42 (1H, dd, J = 8.5 Hz, J = 2.1 Hz), 7.39 (1H, d, J = 8.18 Hz), 7.26–7.28 (2H, m), 2.49 ppm (3H, s); ^{13}C NMR ($CDCl_3$, 100 MHz): δ = 165.36, 159.90, 158.44, 143.56, 138.98, 136.68, 135.62, 134.29, 131.78, 131.31, 131.15, 130.75, 129.98, 129.03 (2C), 127.87, 127.64, 127.21 (2C), 121.23, 114.38, 112.35, 109.13, 29.70, 17.86 ppm; Anal. calcd for $C_{25}H_{18}Cl_2N_6$: C 63.43, H 3.83, N 17.75, found: C 63.45, H 3.79, N 17.76; HRMS (EI): *m/z* $[M]^+$ calcd for $C_{25}H_{18}Cl_2N_6$: 472.0970, found: 472.0972.

Molecular modeling

The computation was carried out in Schrödinger[18] molecular modeling software, which was installed on an Intel Xeon L5420 (2.50 GHz) workstation, with a Linux operating system (FC13).[19] All the ligands were built using the builder interface of Maestro 9.0 and subjected to the LigPrep module (version 23211). LigPrep was set to produce a single low-energy 3D structure with correct chiralities (Force Field OPLS 2005) and multiple protonation/tautomerization states at pH 7.0 ± 2.0 (Epik version 2.0211). The coordinates for the Abl–imatinib complex (PDB ID: 1IEP)[13] were downloaded from the RCSB Protein Data Bank.[20] The protein was then prepared for subsequent grid generation and docking using the Protein Preparation Wizard tool.

Using this tool, the B-chain was removed. All hydrogen atoms were added on the A-chain, and the protonation states for histidine residues were optimized. All crystallographic waters were deleted, and the entire chain was minimized (RMSD = 0.30 Å, Force Field OPLS 2005). Molecular docking studies were performed using the Extra Precision Glide (XP) (version 55212). The docking protocol was validated by reproducing the binding mode of imatinib in the A-chain of the Abl crystal structure (PDB ID: 1IEP). A grid for docking was prepared using the Receptor Grid Generation tool in Glide. Imatinib ligand co-crystallized in the A-chain was chosen as centroid to define the grid box. The option "dock ligands similar in size to the workspace ligand" was selected for determining the grid sizing. For docking, the extra precision mode was selected. The default settings for scaling the van der Waals radii were selected: a scaling factor of 0.8 and a partial charge cutoff of 0.25. No constraints were defined for the docking runs. Finally, the option "Add Epik state penalties to docking score" was selected. The molecules were subjected to predict the pharmacokinetic or ADME properties using the QikProp module (version 32212). All images were generated with PyMOL[21] software (version 1.2.x) and with PoseView Web[22].

Biology

Enzyme assays: Recombinant human Abl was purchased from Upstate Biotechnology (Waltham, MA, USA). Activity was measured in a filter-binding assay using an Abl-specific peptide substrate (Abltide, Upstate Biotechnology). Reaction were incubated for 15 min at 30 °C, in 8 mM MOPS-NaOH pH 7.0, 1 mM EDTA, 25 mM MgOAc, 20 μM ATP, 0.012 μM [γ-^{32}P]ATP, 50 μM peptide, 0.005 μM c-Abl. The apparent affinity (K_M) values of the Abl preparation used for its peptide and ATP substrates were determined separately and found to be 1.5 μM and 10 μM, respectively. Each experiment was done in triplicate, and mean values were used for the interpolation. Curve fitting was performed with the program GraphPad Prism using Equation (1):

$$v = V_{max}/(1 + [I]/IC_{50}) \quad (1)$$

for which v is the reaction rate in the presence of the inhibitor, V_{max} is the apparent maximal reaction rate in the absence of inhibitor, and [I] is the inhibitor concentration.

Cell culture: Human chronic myeloid leukemia (CML) K-562 cells in blast crisis,[23] the human CML MEG-01 cell line in megakaryocytic blast crisis,[24] and the human CML KU-812[25] cell line in myeloid blast crisis were obtained from the American Type Culture Collection. The three cell lines were selected for their different origins, as the K-562 line has been characterized as highly undifferentiated cells of the granulocytic series, whereas the KU-812 line has some characteristics of basophilic leukocytes, and the MEG-01 line is originated from megakaryocytes. Nevertheless, all contain at least one Philadelphia chromosome. Cells were grown in RPMI 1640 medium (Euroclone, Devon, UK) containing 10% fetal bovine serum (FBS) or 20% FBS for KU-812, and antibiotics (100 U mL^{-1} penicillin and 100 μg mL^{-1} streptomycin). The cultures were free of mycoplasma.

Resazurin assay: The resazurin assay (Acros Organics, Geel, Belgium) was used to determine cell proliferation.[26] Starved cells (1×10^4 cells per well) were plated in 96-well plates with RPMI containing FBS, with or without various concentrations (0.05–150 μM) of the studied compounds. Resazurin was dissolved in sterile water and added to the wells 6 h before the term of 72 h incubation, in amounts equal to 5% volume and at a concentration of 320 μM. Resazurin reduction was determined by measuring fluorescence at λ_{ex} 530 nm and λ_{em} 590 nm using FLUOstar Optima (BMG Labtech, Offenburg, Germany). Data analysis for IC_{50} calculations was performed with the L5W Data Analysis Package plug-in for Excel (Microsoft). Results are reported as mean ± SEM.

Western blot analysis: The inhibitory effect of compounds toward the phosphorylation of Bcr-Abl (Tyr 245) and STAT-5 (Tyr 694) were tested using a PathScan Multiplex Western Detection Kit (Cell Sig-

naling Technology, Beverly, MA, USA). This kit was used to assay the inhibition of multiple proteins on membrane without stripping and re-probing. The inhibitory effect toward phosphorylation of Src (Tyr416) was assessed using specific antibody (Cell Signaling Technology). Cells were cultured at a concentration of 1×10^6 cells per well and challenged with FA030 (50, 10, and 1 μM) and reference compound imatinib (1 μM). After 3 h, cells were harvested and lysed in an appropriate buffer containing 1% Triton X-100. Filters were additionally re-probed with β-actin (control loading, Cell Signaling Technology). The pro-apoptotic activity of the selected compounds was also tested, using immunoblot analysis with poly-(ADP-ribose) polymerase (PARP)-specific antibody, which reveals both uncleaved (113 kDa) and cleaved (89 kDa) forms of PARP (Cell Signaling Technology). Cell lines were cultured at a concentration of 14×10^5 cells per well and challenged with various concentrations of the studied compound or control compound, for 72 h. Proteins were quantified by the BCA method (Pierce, Rockford, IL). Equal amounts of total cellular protein were resolved by SDS-polyacrylamide gel electrophoresis, transferred to PVDF filters, and subjected to immunoblot. Non-saturated, immunoreactive bands were detected with a CCD camera gel documentation system (Chemi-DocXRS, Bio-Rad Laboratories, Hercules, CA, USA) and then quantified with Quantity One (Bio-Rad Laboratories).

RNA preparation and qRT-PCR: The mRNA expression of apoptotic genes and proliferation marker genes was performed using qRT-PCR. Cells were cultured and challenged with the compound for 3 (5×10^5 cells per well) or 24 h (7×10^5 cells per well). The cells were then harvested and lysed in appropriate buffer (TRI Reagent®, Ambion, Austin, TX, USA). The extract was processed for extraction of mRNA. First-strand cDNA synthesis was performed using an iScript cDNA Synthesis Kit (Bio-Rad Laboratories). qRT-PCR was performed using iTaq SYBR Green Supermix with Rox (Bio-Rad Laboratories), and specific primers were designed using the PRIMER3 program (available at http://frodo.wi.mit.edu). The expression of cdc25A, Bax, and Bcl-xl was analyzed quantitatively with an iQ™5 Multicolor Real-Time PCR Detection System (Bio-Rad Laboratories). Data were quantitatively analyzed on iQ™5 Optical System Software (Bio-Rad Laboratories). Relative quantification was done by using the $2^{-\Delta\Delta CT}$ method, as previously described;[27] β-actin was used as housekeeping gene, and results were reported as mRNA expression versus control cells.

Statistical analysis: Data are presented as means ± SEM. Statistical significance between means was determined using Student's *t* test. The Bonferroni's correction was used for multiple *t* test comparisons. Data analysis for IC_{50} calculations was performed by the L5W Data Analysis Package plug-in for Excel (Microsoft) as previously described.[5a]

Acknowledgements

This research was developed under the umbrella of CM0602 COST Action "Inhibitors of Angiogenesis: Design, Synthesis and Biological Exploitation". This study was supported by the Associazione Ricerche sul Cancro and Ministero dell'Istruzione, dell'Università e della Ricerca (MIUR) PRIN 2007—Program "Sviluppo e caratterizzazione di nuovi inibitori di tirosine chinasi cellulari con attività antiproliferativa e antiangiogenica nei confronti di differenti tumori". The authors express their gratitude to Novartis for supplying imatinib as a reference compound.

Keywords: Bcr-Abl · CuAAC · imatinib · inhibitors · leukemia · triazoles

[1] P. C. Nowell, D. A. Hungerford, *Science* **1960**, *132*, 1497 – 1501.
[2] J. D. Rowley, *Nature* **1973**, *243*, 290 – 293.
[3] C. L. Sawyers, *N. Engl. J. Med.* **1999**, *340*, 1330 – 1340.
[4] T. G. Lugo, A. M. Pendergast, A. J. Muller, O. N. Witte, *Science* **1990**, *247*, 1079 – 1082.
[5] a) F. Manetti, C. Brullo, M. Magnani, F. Mosci, B. Chelli, E. Crespan, S. Schenone, A. Naldini, O. Bruno, M. L. Trincavelli, G. Maga, F. Carraro, C. Martini, F. Bondavalli, M. Botta, *J. Med. Chem.* **2008**, *51*, 1252 – 1259; b) F. Manetti, A. Pucci, M. Magnani, G. A. Locatelli, C. Brullo, A. Naldini, S. Schenone, G. Maga, F. Carraro, M. Botta, *ChemMedChem* **2007**, *2*, 343 – 353; c) C. Walz, M. Sattler, *Crit. Rev. Oncol. Hematol.* **2006**, *57*, 145 – 164; d) W. Huang, C. Metcalf, R. Sundaramoorthi, Y. Wang, D. Zou, R. Thomas, X. Zhu, L. Cai, D. Wen, S. Liu, J. Romero, J. Qi, I. Chen, G. Banda, S. Lentini, S. Das, Q. Xu, J. Keats, F. Wang, S. Wardwell, Y. Ning, J. Snodgrass, M. Broudy, K. Russian, T. Zhou, L. Commodore, N. Narasimhan, Q. Mohemmad, J. Iuliucci, V. Rivera, D. Dalgarno, T. Sawyer, T. Clackson, W. Shakespeare, *J. Med. Chem.* **2010**, *53*, 4701 – 4719 and references therein; e) D. Wang, Z. Zhang, X. Lu, Y. Feng, K. Luo, J. Gan, L. Yingxue, J. Wana, X. Li, F. Zhang, Z. Tu, Q. Cai, X. Ren, K. Ding, *Bioorg. Med. Chem.* **2011**, *21*, 1965 – 1968 and references therein.
[6] S. Schenone, O. Bruno, M. Radi, M. Botta, *Med. Research Reviews* **2011**, *31*, 1 – 41.
[7] a) J. Zimmermann, E. Buchdunger, H. Mett, T. Meyer, N. B. Lydon, *Bioorg. Med. Chem. Lett.* **1997**, *7*, 187 – 192; b) T. Schindler, W. Bornmann, P. Pellicena, W. T. Miller, B. Clarkson, J. Kuriyan, *Science* **2000**, *289*, 1938 – 1942.
[8] For other syntheses of Abl inhibitors using click chemistry, see: K. A. Kalesh, K. Liu, S. Q. Yao, *Org. Biomol. Chem.* **2009**, *7*, 5129 – 5136.
[9] E. D. Chrysina, E. Bokor, K. Elexacou, M. Charavgi, G. N. Oikonomakos, S. E. Zographos, D. D. leonidas, N. G. Oikonomakos, L. Somsàk, *Tetrahedron: Asymmetry* **2009**, *20*, 733 – 740.
[10] M. Meldal, C. W. Tornoe, *Chem. Rev.* **2008**, *108*, 2952 – 3015.
[11] Y. F. Liu, C. L. Wang, Y. J. Bai, N. Han, J. P. Jiao, X. L. Qi, *Org. Process Res. Dev.* **2008**, *12*, 490 – 495.
[12] S. Ohira, *Synth. Commun.* **1989**, *19*, 561 – 564.
[13] M. Warmuth, R. Damoiseaux, Y. Liu, D. Fabbro, N. Gray, *Curr. Pharm. Des.* **2003**, *9*, 2043.
[14] X. Zou, S. Rudchenko, K. Wong, K. Calame, *Genes Dev.* **1997**, *11*, 654 – 62.
[15] K. Kristjánsdóttir, J. Rudolph, *Chem. Biol.* **2004**, *11*, 10431051.
[16] B. Nagar, W. G. Bornmann, P. Pellicena, T. Schindler, D. R. Veach, W. T. Miller, B. Clarkson, J. Kuriyan, *Cancer Res.* **2002**, *62*, 4236 – 43.
[17] M. Radi, E. Crespan, F. Falchi, V. Bernardo, S. Zanoli, F. Manetti, S. Schenone, G. Maga, M. Botta, *ChemMedChem* **2010**, *5*, 1226 – 1231.
[18] Schrödinger Molecular Modeling Platform: http://www.schrodinger.com/ (accessed August 5, 2011).
[19] Fedora: http://fedoraproject.org/ (accessed August 5, 2011).
[20] RCSB Protein Data Bank (PDB): http://www.rcsb.org/pdb/ (accessed August 5, 2011).
[21] PyMOL Molecular Visualization Software: http://www.pymol.org/ (accessed August 5, 2011).
[22] The PoseView Project, Center for Bioinformatics, University of Hamburg (Germany): http://poseview.zbh.uni-hamburg.de (accessed August 5, 2011).
[23] D. Hudig, M. Djobadze, D. Redelman, J. Mendelsohn, *Cancer Res.* **1981**, *41*, 2803 – 2808.
[24] M. Ogura, Y. Morishima, R. Ohno, Y. Kato, N. Hirabayashi, H. Nagura, H. Saito, *Blood* **1985**, *66*, 1384 – 1392.
[25] K. Kishi, *Leuk. Res.* **1985**, *9*, 381 – 390.
[26] M. K. McMillian, L. Li, J. B. Parker, L. Patel, Z. Zhong, J. W. Gunnett, W. J. Powers, M. D. Johnson, *Cell. Biol. Toxicol.* **2002**, *18*, 157 – 173.
[27] J. Vandesompele, P. K. De, F. Pattyn, B. Poppe, R. N. Van, P. A. De, F. Speleman, *Genome Biol.* **2002**, *3*, research0034.1 – research0034.11.

Received: March 29, 2011
Revised: August 2, 2011
Published online on August 30, 2011

